AN INVESTIGATION OF THE OXIDATION OF LASER AND FURNACE-ANNEALED SPUTTER-DEPOSITED NI-TI THIN FILMS USING REFLECTIVITY MEASUREMENTS

Fadila Khelfaoui[1], Yves Bellouard[2], Thomas Gessmann[2], Xi Wang[3], Joost Vlassak[3], Moustapha Hafez[1]

[1]French Atomic Energy Commission (CEA LIST), 18 Route du Panorama, 92265 Fontenay-aux-Roses, France
[2]Rensselaer Polytechnic Institute, 110, 8th Street, Troy, NY, 12180-3590 USA
[3]Harvard University, 40 Oxford Street, Cambridge, MA 02138 USA

ABSTRACT

Shape Memory Alloy (SMA) thin films are of particular interest as micro-actuators. Thus far, their use in microsystems is still limited due to numerous technological issues that have yet to be overcome. In particular, film oxidation during annealing has to be carefully controlled to preserve the material properties. In Ni-Ti thin films, the oxide layer can make up a significant fraction of the total film thickness. Native oxides like TiO_2 rapidly form on Ni-Ti alloy surfaces in the presence of oxygen. The oxide layer thickness depends on annealing conditions (i.e. temperature, time and atmosphere). During the oxidation process, compositional changes may occur in the Ni-Ti film. Hence, the properties of the film can be significantly altered and the martensitic transformation reduced or even inhibited. In this paper, we present a study of oxide growth on Ni-Ti thin films. Oxide thickness measurements were performed using optical reflectometry. Thin films were deposited on fused quartz substrates using magnetron sputtering in a UHV chamber with confocal sputter guns. Films of three different compositions - near equiatomic and Ti-rich - were considered. The as-deposited amorphous films were heat treated using either furnace or laser annealing. We compare the two methods in terms of oxide growth kinetics and discuss the influence of film composition.

INTRODUCTION

Thanks to their shape memory and superelastic properties, Ni-Ti thin films are of particular interest for application in microsystems [1]. Shape memory and superelastic properties are only observed in crystalline films that undergo a thermoelastic martensitic phase transformation. Sputter-deposited films are usually deposited at room temperature and are amorphous as-deposited. Heat treatments to crystallize the films can be performed in-situ in the deposition chamber or in a furnace under high vacuum conditions to prevent oxidation. To fully exploit thin-film SMA properties and, in particular, to integrate a two-way shape memory effect, it would be desirable to have shape memory in certain areas of the film and not in others. Bellouard *et al.* [2] have demonstrated that this can be achieved by selectively annealing certain areas of the film. Among the various methods that have been proposed, laser annealing [2, 3] is the most promising: it is a flexible process, it is easy to implement and unlike annealing techniques based on Joule heating it does not require any particular geometry. Heating is done locally, at the point where the laser beam is focused. Depending on how sophisticated the focusing optic is, this zone can be almost as small as the dimension of the laser wavelength. Although the heating time is several orders of magnitude shorter than for furnace annealing, the laser annealing process still results in the formation of an oxide

layer on the surface of the film [3]. The thickness of this layer may represent a significant fraction of the original film thickness. Depending on annealing conditions and film thickness, the oxide layer could significantly modify or even completely inhibit the phase transformation characteristics. It is therefore essential to investigate the oxide growth kinetics in thin films. Oxidation phenomena in bulk furnace-annealed Ni-Ti alloys have been studied by many authors [4-6] as a possible means to improve the corrosion resistance of the alloys. The purpose of the present investigation is to measure the oxide growth on both laser-annealed and furnace-annealed Ni-Ti thin films. All films are annealed in air (natural convection) and oxide thicknesses are determined from reflectivity measurements.

EXPERIMENTAL PROCEDURE

Three sets of films with a thickness of approximately 1.5 μm were deposited onto fused quartz substrates using UHV magnetron sputtering. The films compositions are shown in Table 1.

	Films A (Nearly equi-atomic)	Films B (Ti-Rich)	Films C (Ti-Rich)
Ti (at. %)	50.5	52.8	54.5

***Table 1**: Ni-Ti films composition as determined by electron microprobe analysis.*

Specimens were furnace-annealed at two different temperatures (380°C and 500°C) for time periods ranging from 5 to 90 minutes. Cooling was performed under free air condition. Local laser annealing was performed by scanning a continuous wave (CW) near-infrared laser beam operating at 980 nm on a specimen to generate an array of parallel line with a spacing of 0.2 mm. Scanning speeds ranging from 1 to 4 mm/sec and various optical power densities were used. The laser beam spot size was 1.29 mm. Reflectivity measurements were carried out at room temperature using a spectrophotometer (JascoV-570 NUV/VIS/NIR) under near-vertical incidence over spectral range from 200 to 2500 nm. Oxide thicknesses were calculated from the reflectivity spectrum. The calculation method described by Manifacier *et al.* [7], consists of evaluating the oxide thickness by locating minima induced by destructive optical interference in the reflectivity spectrum. The method is briefly summarized below. For a non-absorbing medium and normal incidence, the reflectivity R of an oxide layer bounded by two media, i.e., air and Ni-Ti, is given by

$$R = \frac{\left(r_1^2 + 2r_1r_2\cos 2\delta + r_2^2\right)}{\left(1 + 2r_1r_2\cos 2\delta + r_1^2r_2^2\right)}, \qquad (1)$$

where, r_1 and r_2 are the reflection coefficients of the upper and lower interface, respectively. δ is the optical path difference and is expressed by:

$$\delta = \frac{2\pi}{\lambda} nx, \qquad (2)$$

where n and x are the refractive index and the thickness of the oxide layer, respectively, and λ is the wavelength. As a result of constructive and destructive interference, the reflectance spectrum presents alternating maxima and minima that occur when the following condition is satisfied:

$$\frac{4\pi\lambda x}{\lambda} = m\pi \begin{cases} m = 2k & \max \\ m = 2k+1 & \min \end{cases} \quad k \text{ and } m \in \mathbb{N}, \qquad (3)$$

where m is the order of the extremum. The oxide thickness x can be calculated from two maxima or minima with order numbers m_1 and m_2, using the following equation [7]:

$$x = \frac{M\lambda_1\lambda_2}{2\left(n(\lambda_1)\lambda_2 - n(\lambda_2)\lambda_1\right)}, \qquad (3)$$

where M is the number of oscillations between the two maxima or minima, i.e., $M = (m_2-m_1)/2$. For two consecutive maxima or minima, M is equal to 1. Here, λ_i and n (λ_i) are the wavelength and refractive index of the extremum of order m_i. It is important to note that the refractive index n depends on the wavelength. Therefore, the thickness can only be calculated from the reflectance measurements if the index of refraction is known at the wavelengths corresponding to the extrema in the reflectance spectrum. We have used ellipsometry measurements to measure the index of refraction over the same spectral window as the reflectivity measurements.

EXPERIMENTAL RESULTS

The reflectance spectra of specimens A and C's in the furnace-annealed condition are shown in Fig. 1 (a) and (b), respectively. The spectrum of an amorphous film in the as-deposited conditions is given for comparison. After annealing at 380°C, minima in the reflectance curves are observed. For specimen A, several minima are found which denotes the presence of a thicker oxide compared to specimens B and C. The laser-annealed films show a similar behavior for all three chemical compositions (Fig. 1 (c) and (d)), although fewer reflectance minima are observed when the power density decreases and/or the scan speed increases.

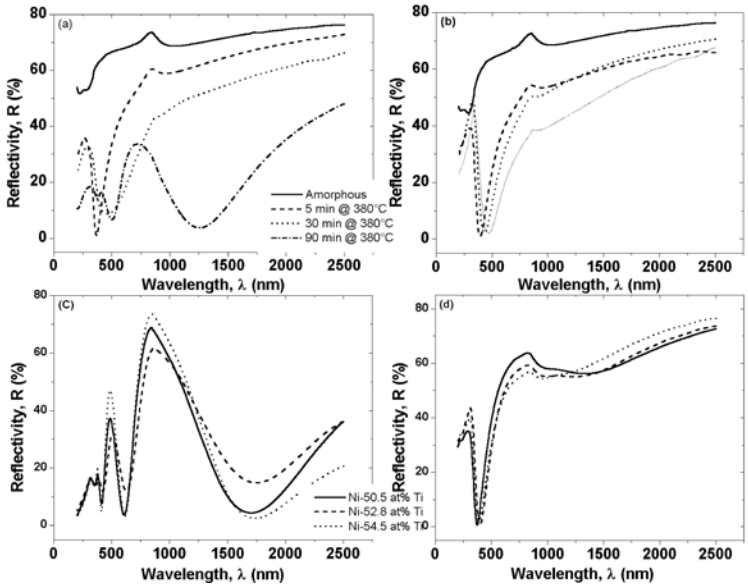

Fig. 1: *Reflectivity spectrum of amorphous and 380°C furnace-annealed films (a) Ni-50.5 at% Ti, (b) Ni-54.5at% Ti, (c) Laser-annealed films at 6.26 W/mm^2 with 2 mm/sec, (d) Laser-annealed films 6.26 W/mm^2 with 4 mm/sec.*

Oxide thicknesses were calculated using Equation (3) and are shown in Fig. 2 and 3, for furnace and laser-annealed specimens respectively. For furnace-annealed specimens, Fig. 2 clearly illustrates that different oxide growth behaviors are observed depending on the composition of the films.

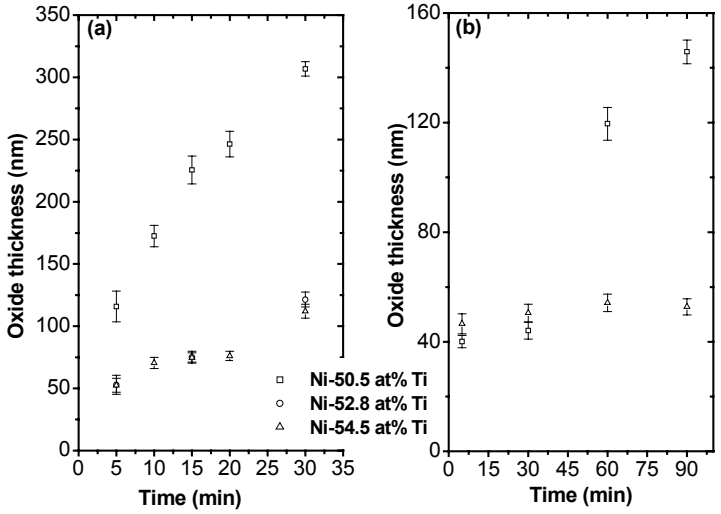

Fig. 2: *Oxide thicknesses versus annealing time for two different annealing temperatures: (a) 500°C, (b) 380°C.*

Relatively fast oxide growth is observed for specimens A with nearly equi-atomic composition; Ti-rich films, (specimens B and C), on the other hand, show a much slower increase of the oxide thickness with time. The oxide growth curves were fit using parabolic ($x^2 \approx k_x t$) and/or logarithmic ($x \approx k_{log} \log(t) + A$) growth laws [6]. Nearly equi-atomic Ni-Ti films (specimens A) are best described by the parabolic law, while Ti-rich films (specimens B and C) follow the logarithmic law. The oxide growth behavior of Ti-rich films is the same at both temperatures. By contrast, the equiatomic films show a sudden increase in oxide thickness when annealed at 380°C for more than 30 minutes. This sudden increase seems to be associated with a transition from a logarithmic to parabolic growth law. At 500°C, the parabolic growth law is observed from the very first measurement.

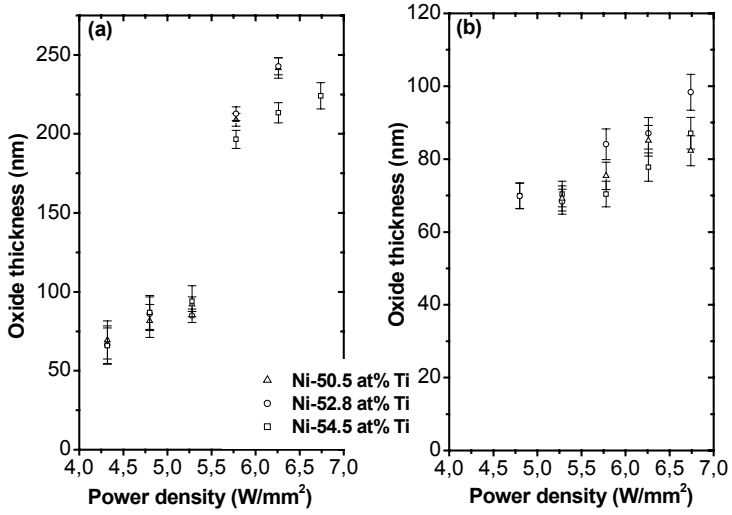

Fig. 3: *Oxide thicknesses versus power density for two laser-scan speeds, (a) 2 mm/sec, (b) 4 mm/sec.*

The oxide thickness growth for laser-annealed specimens is presented in Fig. 3. For power densities ranging from 4.32 to 5.28 W/mm^2 with a laser-scan speed of 2 mm/sec, a linear oxide growth is observed first. The maximum thickness for this linear regime is less than 100 nm. If the power density is increased further, the oxide thickness increases suddenly. The discontinuity in the growth rate shown in Fig. 3a is similar to that observed for furnace-annealed equiatomic films at 380°C (see Fig. 2b). Furthermore, Fig. 3 shows that for a laser scan speed of 2 mm/sec, the same oxide growth rate behavior is observed for the three different films compositions. Similar behavior is also observed for 3 mm/sec laser-scan speed (not shown). For relatively higher scan speed as 4 mm/sec (Fig. 3b), the oxide thickness seems to increase linearly over the range of power density explored. This behavior is observed independent of the chemical composition of the films.

DISCUSSION

The oxidation behavior of furnace-annealed Ni-Ti thin films depends both on composition and annealing temperature. For specimens A, which were heat treated for less than 30 minutes, the oxide growth changes from logarithmic to parabolic when the temperature is increased from 380 to 500°C. Both oxygen ion and metal ion diffusion are involved in oxide growth. Due to the difference in activation energy, oxygen ion diffusion through the oxide layer is predominant at low temperature, while diffusion of metal ions determines the rate at higher temperatures. This accounts for the transition from logarithmic to parabolic growth with increasing temperature [6, 9]. The growth rate for specimen A, furnace-annealed at 500°C, shown in Fig. 2 (a), is in the same order of magnitude as the one of an equiatomic Ti-Ni bulk alloy annealed at temperature ranging from 550°C to 750°C observed by Xu *et al*. [6]. The authors suggest a parabolic growth rate which is in agreement with our results. The more interesting observation is a transition from logarithmic to parabolic growth that occurs at 380^{o}C when the films are heat-treated for more than 30 minutes and the oxidation rate increases as well. This transition is likely to be related to the nature of the electric field that develops in the growing oxide film as described by the Cabrera-Mott theory for thin films and Wagner theory for thick films [14]. Logarithmic oxidation growth takes place by an inward diffusion mechanism [9]. Since titanium has a higher oxidation potential than Nickel [10], an oxide layer mainly of rutile (TiO_2) grows on the Ni-Ti film surface [8, 11]. At lower temperatures, the oxygen ions diffusion in TiO_2 is predominant. With increasing temperature and/or time exposure, the TiO_2 oxide thickens. Once the TiO_2 oxide layer reaches a critical thickness, the Ti diffusion length increases and an outward diffusion mechanism takes place. This mechanism is associated with a parabolic growth rate [4, 6, 9]. This mechanism, however, does not explain why the oxidation rate increases after 30 minutes heat treatment. A possible explanation is the decomposition of Ti oxide by the neighboring metallic Ti at the oxide-alloy interface according to Bui *et al.* [16]. They found that this decomposition happens during oxidation at temperatures above 350^{o}C and that it creates a high density of vacancies, which can improve the oxygen diffusion and result in an increase of the oxidation rate. Within the time-scale studied, Ti-rich specimens show logarithmic growth at both 380 and 500^{o}C and the oxide thickness is smaller than for near equi-atomic films. A possible explanation is that different oxide compounds, like Ti_4Ni_2O, form in the Ti-rich specimen with different diffusion and oxide kinetics as a result. Laser-induced oxidation is more complicated than isothermal furnace oxidation due to the intrinsic nonlinearity of optical, chemical and thermal properties of the irradiated solid and the reaction products [13]. In this study, similar oxide growth behavior is observed for all the three different compositions. This may indicate that the same oxide compounds are formed by laser irradiation

regardless of the chemical composition. Furthermore, the oxide thickness increases steeply near the corresponding critical laser power density for different scan speed and this transition shifts toward high power with increasing scan speed. It should also be noted that the discontinuity happens at the oxide thickness about 100 nm independent of laser power and scan speed. A possible explanation is a local temperature rise resulting from a sudden increase of the film absorptivity and/or a change in the oxide optical properties. Consequently a rate enhancement occurs. According to a study of laser induced amorphous Ti_2O_3 growth by Merlin and Perry [15], an increase of the absorbed power from 45% to 80% happens around 100 nm oxide thickness for a CW Krypton green laser. From the above, we can see that for comparable oxide thickness, oxide growth occurs much faster in laser annealing than in furnace annealing. This would imply that for laser annealing the temperature is higher recalling the activation-type temperature dependence of the reaction rate, i.e. $w \propto exp(-Q/RT)$.

CONCLUSIONS

Oxide growth in furnace and laser annealed sputter-deposited thin films were studied using reflectivity measurements. For furnace-annealed specimens, two growth mechanisms were observed for specimens annealed at 380°C and 500°C. Oxide growth in Ti-rich films followed a logarithmic law for both annealing temperatures while equiatomic specimens exhibited two-stages oxide growths behavior characterized by a logarithmic/parabolic law transition. We explain this particular behavior by a phenomenological model that describes the oxidation mechanisms. For laser-annealed specimens, a similar oxide growth behavior was observed for all films compositions (equiatomic and Ti-rich).

REFERENCES

[1] Y. Fu, H. Du, W. Huang, S. Zhang, M. Hu, in Sensors and Actuators A 112, (2004), 395.
[2] Y. Bellouard, T. Lehnert, J.-E. Bidaux, T. Sidler, R. Clavel, R. Gotthardt, in Materials Science and Engineering A 273-275, (1999), 795.
[3] Y. Bellouard, T. Lehnert, R. Claver T. Sidler, R. Gotthardt, in Journal de Physique 11, (2000), C8-571.
[4] C.L. Chu, S.K. Wu, Y.C. Yen, in Science and Engineering A 216, (1996), 193.
[5] G.S. Firstov, R.G. Vitchev, H. Kumar, B. Blanpain, J. Van Humbeeck, in Biomaterials 23, (2002), 4863.
[6] C.H. Xu, X.Q. Ma, S.Q. Shi, C.H. Woo, in Materials Science and Engineering A 371, (2004), 45.
[7] J.C. Manifacier, J. Gasiot, J.P. Fillard, in Journal of Physics E: Scientific Instruments 9, (1976), 1002.
[8] C.M. Chan, S. Trigwell, T. Dyerig, in Surface and Interface analysis 15, (1990), 349.
[9] D.A. Armitage, D.M. Grant, in Materials Science and Engineering A 349, (2003), 89.
[10] S. Barison, S. Cattarin S. Daolio, M. Musiani, A. Tsuissi, in Electrochimica Acta, to be published.
[11] E. Rówiński, in Surface Science 411, (1998), 316.
[12] K. R. Lawless, in Reports on Progress in Physics 37, (1974), 231.
[13] L. Nánai, R. Vajtai, T. F. George, in Thin Solid Films 298, (1997), 160.
[14] A. Atkinson, in Reviews of Modern Physics, 57(2), (1985), 437.
[15] R. Merlin, T.A. Perry, in Applied Physics Letters, 45(8), (1984), 852.
[16] M. D. Bui, C. Jardin, J. P. Gauthier, G. Thollet, P. Michel, in Titanium ’80: Proceedings of the Fourth International Conference on Titanium, Kyoto, vol. 4, (1980), 2821.